

1 Supporting Information for:

2 **Trans-Basin Interaction Sustains Multi-Year Marine Heatwaves**  
3 **in the Gulf of Alaska**

4 Yu Zhao<sup>1</sup>, Jin-Yi Yu<sup>1\*</sup>, Huang-Hsiung Hsu<sup>2</sup>, I-I Lin<sup>3</sup>, Song Yang<sup>4,5</sup>, Chunzai Wang<sup>6,7,8</sup>,  
5 Jian Shi<sup>9,10</sup>, Yan Du<sup>11</sup>, Xin Wang<sup>6,7</sup>, Tao Lian<sup>12</sup>, and Sang-Wook Yeh<sup>13</sup>

6 <sup>1</sup> *Department of Earth System Science, University of California, Irvine, CA, USA.*

7 <sup>2</sup> *Research Center for Environmental Changes, Academia Sinica, Taipei, Taiwan*

8 <sup>3</sup> *Department of Atmospheric Sciences, National Taiwan University, Taipei, Taiwan*

9 <sup>4</sup> *School of Atmospheric Sciences, Sun Yat-sen University, and Southern Marine Science and*  
10 *Engineering Guangdong Laboratory (Zhuhai), Zhuhai, China*

11 <sup>5</sup> *Guangdong Province Key Laboratory for Climate Change and Natural Disaster Studies, Sun Yat-sen*  
12 *University, Zhuhai, China*

13 <sup>6</sup> *State Key Laboratory of Tropical Oceanography, South China Sea Institute of Oceanology, Chinese*  
14 *Academy of Sciences, Guangzhou, China*

15 <sup>7</sup> *Global Ocean and Climate Research Center, South China Sea Institute of Oceanology, Chinese*  
16 *Academy of Sciences, Guangzhou, China*

17 <sup>8</sup> *Guangdong Key Laboratory of Ocean Remote Sensing, South China Sea Institute of Oceanology,*  
18 *Chinese Academy of Sciences, Guangzhou, China*

19 <sup>9</sup> *Frontier Science Center for Deep Ocean Multispheres and Earth System (FDOMES) and Physical*  
20 *Oceanography Laboratory, Ocean University of China, Qingdao, China*

21 <sup>10</sup> *College of Oceanic and Atmospheric Sciences, Ocean University of China, Qingdao, China*

22 <sup>11</sup> *Guangdong Key Laboratory of Ocean Remote Sensing, State Key Laboratory of Tropical*  
23 *Oceanography, South China Sea Institute of Oceanology, Chinese Academy of Sciences, Guangzhou,*  
24 *China*

25 <sup>12</sup> *State Key Laboratory of Satellite Ocean Environment Dynamics, Second Institute of Oceanography,*  
26 *Ministry of Natural Resources, Hangzhou, China*

27 <sup>13</sup> *Department of Marine Science and Convergence Engineering, Hanyang University, ERICA, Ansan,*  
28 *Republic of Korea*

29 \*Corresponding authors: Jin-Yi Yu ([jyyu@uci.edu](mailto:jyyu@uci.edu))

30

31 **This Supplementary Information file includes:**

32 • **Tables S1 to S3**

33 • **Figures S1 to S9**

34 **Table S1. Granger Causality Test Results.** Results show the exclusion tests for each variable  
 35 index pairing in a 5-variable Vector Autoregression model with 6-month lags. Tests evaluate  
 36 whether excluding lagged values of one variable significantly affects predictions of another  
 37 (Chi2(6) distribution, critical value=12.592). For example, "Exclude lagged TCP in SEP  
 38 equation" tests whether past TCP values help predict SEP values. Results indicate whether the  
 39 null hypothesis (H0) of no Granger causality can be rejected at  $p < 0.05$ , revealing significant  
 40 causal pathways in the Pacific-Atlantic interaction system.

<i>H0</i>	<i>Decision</i>	<i>p Value</i>
Exclude lagged TCP in SEP equation	Reject H0	0.0000
Exclude lagged WTI in SEP equation	Cannot reject H0	0.9650
Exclude lagged GOA in SEP equation	Cannot reject H0	0.1415
Exclude lagged TNA in SEP equation	Reject H0	0.0022
Exclude lagged SEP in TCP equation	Reject H0	0.0139
Exclude lagged WTI in TCP equation	Cannot reject H0	0.3962
Exclude lagged GOA in TCP equation	Cannot reject H0	0.1547
Exclude lagged TNA in TCP equation	Reject H0	0.0210
Exclude lagged SEP in WTI equation	Reject H0	0.0012
Exclude lagged TCP in WTI equation	Cannot reject H0	0.2829
Exclude lagged GOA in WTI equation	Reject H0	0.0000
Exclude lagged TNA in WTI equation	Cannot reject H0	0.3125
Exclude lagged SEP in GOA equation	Reject H0	0.0333
Exclude lagged TCP in GOA equation	Cannot reject H0	0.2215
Exclude lagged WTI in GOA equation	Reject H0	0.0000
Exclude lagged TNA in GOA equation	Reject H0	0.0055
Exclude lagged SEP in TNA equation	Cannot reject H0	0.0643
Exclude lagged TCP in TNA equation	Reject H0	0.0102
Exclude lagged WTI in TNA equation	Reject H0	0.0000
Exclude lagged GOA in TNA equation	Reject H0	0.0079

41

42

43 **Table S2. Granger Causality Results Across Different Lag Orders.** Results show exclusion  
 44 tests for each variable index pairing using Vector Autoregression models with different lag  
 45 specifications (3-8 months). The table evaluates whether past values of one variable  
 46 significantly improve predictions of another beyond the variable's own history. Statistical  
 47 significance assessed using chi-square tests at  $p < 0.05$  level. "YES" indicates robust causal  
 48 relationships significant across most lag orders; "PARTIAL" indicates relationships significant  
 49 at multiple but not all lags; "NO" indicates consistently non-significant relationships. The core  
 50 trans-basin feedback pathway (SEP  $\rightarrow$  WTI  $\rightarrow$  GOA and WTI  $\rightarrow$  TNA) demonstrates high  
 51 robustness across all tested lag specifications, while Atlantic feedback components (TNA  $\rightarrow$   
 52 SEP/TCP) show moderate lag sensitivity.

<b><i>Causal Relationship</i></b>	<b><i>Lag 3</i></b>	<b><i>Lag 4</i></b>	<b><i>Lag 5</i></b>	<b><i>Lag 6</i></b>	<b><i>Lag 7</i></b>	<b><i>Lag 8</i></b>	<b><i>Robust</i></b>
<i>SEP <math>\rightarrow</math> WTI</i>	√**	√**	√**	√***	√*	√*	YES
<i>WTI <math>\rightarrow</math> GOA</i>	√***	√***	√***	√***	√***	√***	YES
<i>WTI <math>\rightarrow</math> TNA</i>	√***	√***	√***	√***	√***	√***	YES
<i>TNA <math>\rightarrow</math> SEP</i>	X	X	√**	√**	√*	X	PARTIAL
<i>TNA <math>\rightarrow</math> TCP</i>	√**	X	√*	√*	X	X	PARTIAL
<i>TCP <math>\rightarrow</math> WTI</i>	X	X	X	X	X	X	NO

53 √\*\*\*  $p < 0.001$ , √\*\*  $p < 0.01$ , √\*  $p < 0.05$ , X not significant

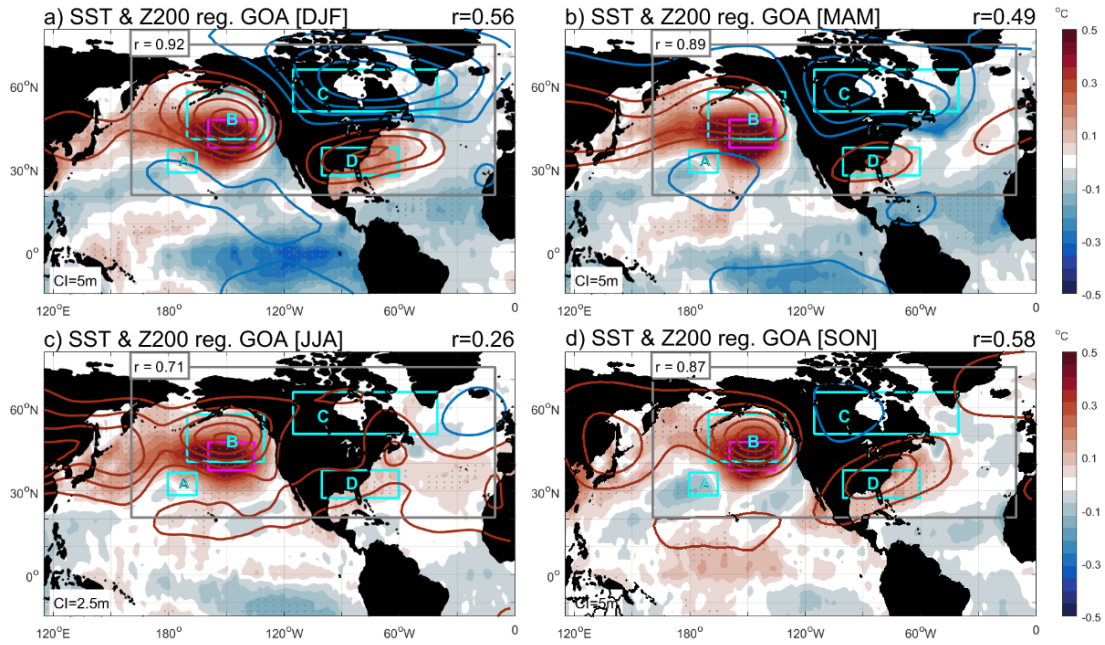
54

55 **Table S3. Multi-year Gulf of Alaska Marine Heatwave (MHW) Periods.** Multi-year MHW  
 56 periods from 1871-2022, where MHWs occurred in at least three out of four consecutive years.  
 57 For each period, the constituent MHW events are detailed, providing their start and end dates.

<i>Period</i>	<i>Individual MHW Episodes</i>
1873-1876	Feb 1873 - Aug 1873
	Jan 1874 - Sep 1874
	Jan 1876 - Sep 1876
1880-1887	Jan 1880 - Sep 1880
	Dec 1880 - May 1881
	Mar 1882 - Sep 1882
	Apr 1883 - Aug 1883
	Jan 1884 - Aug 1884
	Jan 1885 - May 1885
1917-1920	May 1887 - Sep 1887
	Feb 1917 - Jul 1917
	Jan 1918 - Jul 1918
	Feb 1920 - Jul 1920
1949-1952*	Jan 1949 - Oct 1949
	Jan 1950 - Jul 1950
	May 1951 - Sep 1951
1962-1965*	Jan 1962 - Sep 1962
	Jan 1963 - Aug 1963
	Feb 1965 - Aug 1965
1989-1992	Aug 1989 - May 1990
	Dec 1990 - Jan 1992
2013-2016*	Apr 2013 - Aug 2013
	Nov 2013 - Sep 2014
	Feb 2015 - Sep 2015
2018-2022*	May 2019 - Sep 2021
	Jan 2022 - Nov 2022

58 \* Periods analyzed in detail in the main text.

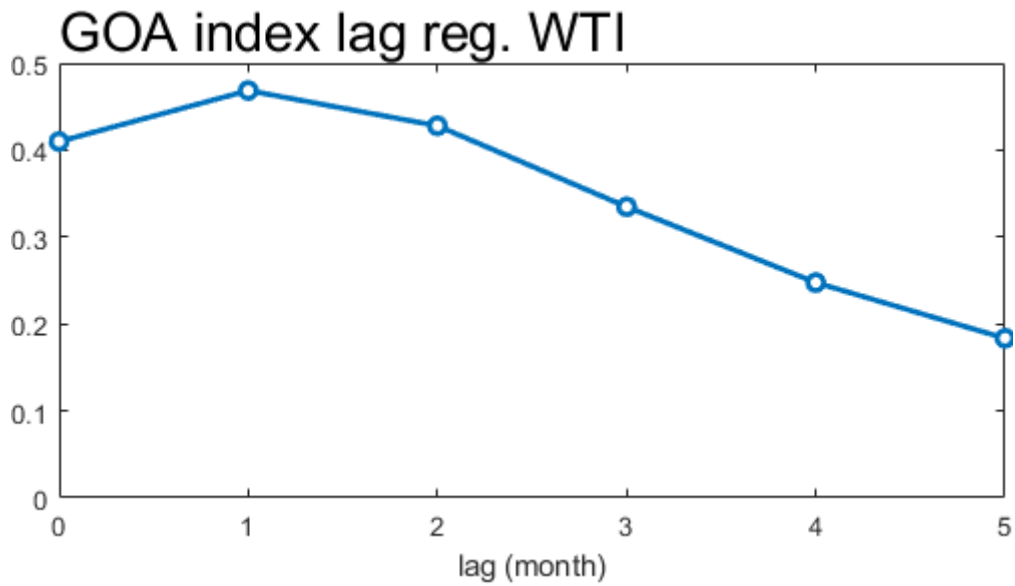
59



60

61 **Figure S1. The trans-basin wave train produces GOA MHWs across all four seasons.** SST  
 62 (shading, °C) and Z200 (contours, m) anomalies regression onto GOA index for DJF, MAM,  
 63 JJA, and SON (a-d). Pattern correlation coefficients ( $r$ ) between each seasonal panel and Figure  
 64 1a, calculated specifically within the highlighted gray box regions, are labeled. Correlations  
 65 between GOA index and WTI (lead by one month) are shown in the upper right of each panel.  
 66 The wave train centers A-D correspond to those identified in Figure 1. Magenta boxes mark  
 67 GOA region. Gray dots show 95% significance for SST.

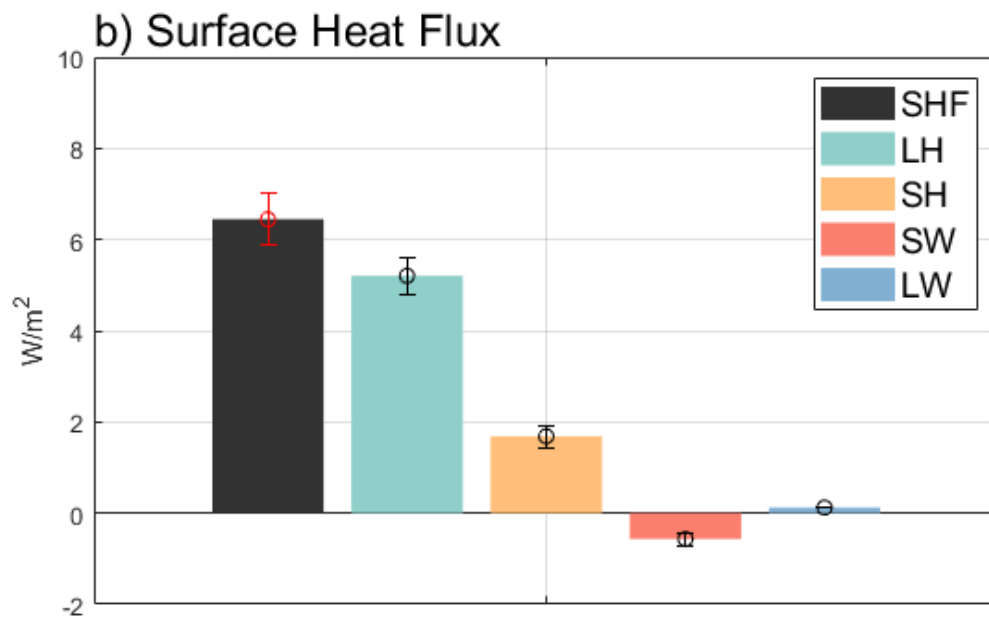
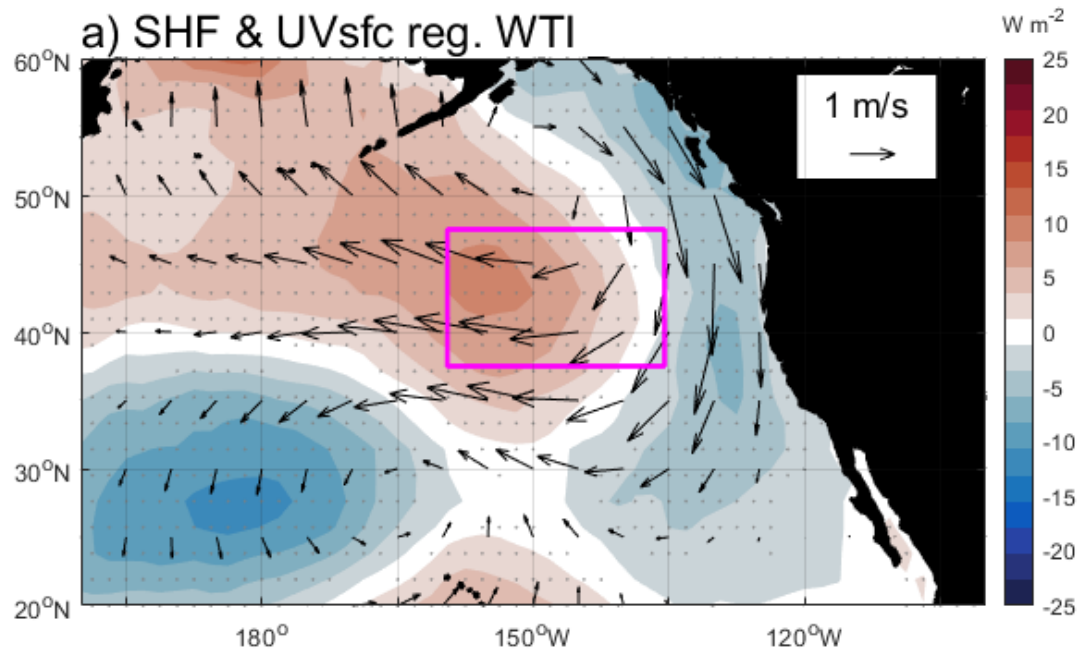
68



69

70 **Figure S2. Lag Sensitivity Analysis for WTI-GOA Correlation.** Lag correlation between the  
71 Wave Train Index (WTI) and the Gulf of Alaska (GOA) index from 1871 to 2022, with lag time  
72 (in months) representing the delay of the GOA index relative to the WTI. The peak correlation  
73 at a 1-month lag supports the selection of this lag as the oceanic response time to atmospheric  
74 forcing.

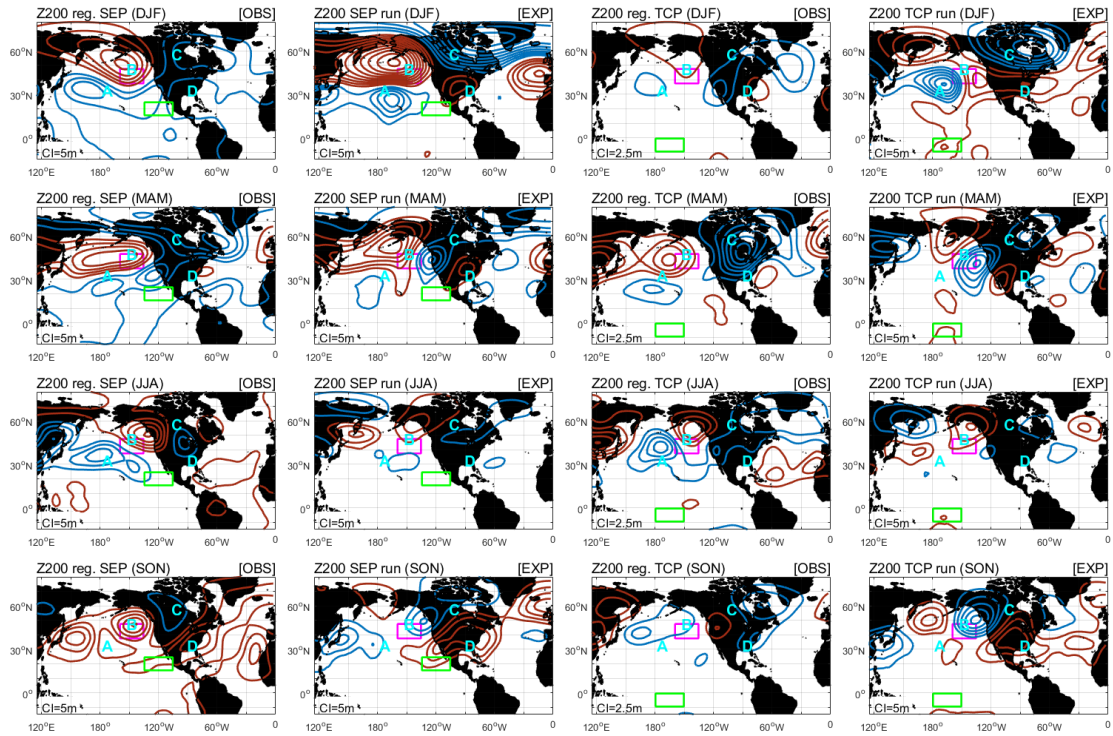
75



76

77 **Figure S3. The trans-basin wave train produces GOA MHWs via Surface Heat Flux.** (a)  
 78 SHF (shading,  $W/m^2$ ) and surface wind (contours, m/s) anomalies regression onto WTI. (b)  
 79 Component contributions to GOA mean SHF: latent heat (LH), sensible heat (SH), shortwave  
 80 radiation (SW), and longwave radiation (LW). Magenta box: GOA region. Gray dots show 95%  
 81 significant SHF in (a). Error bars show the 95% confidence interval in (b).

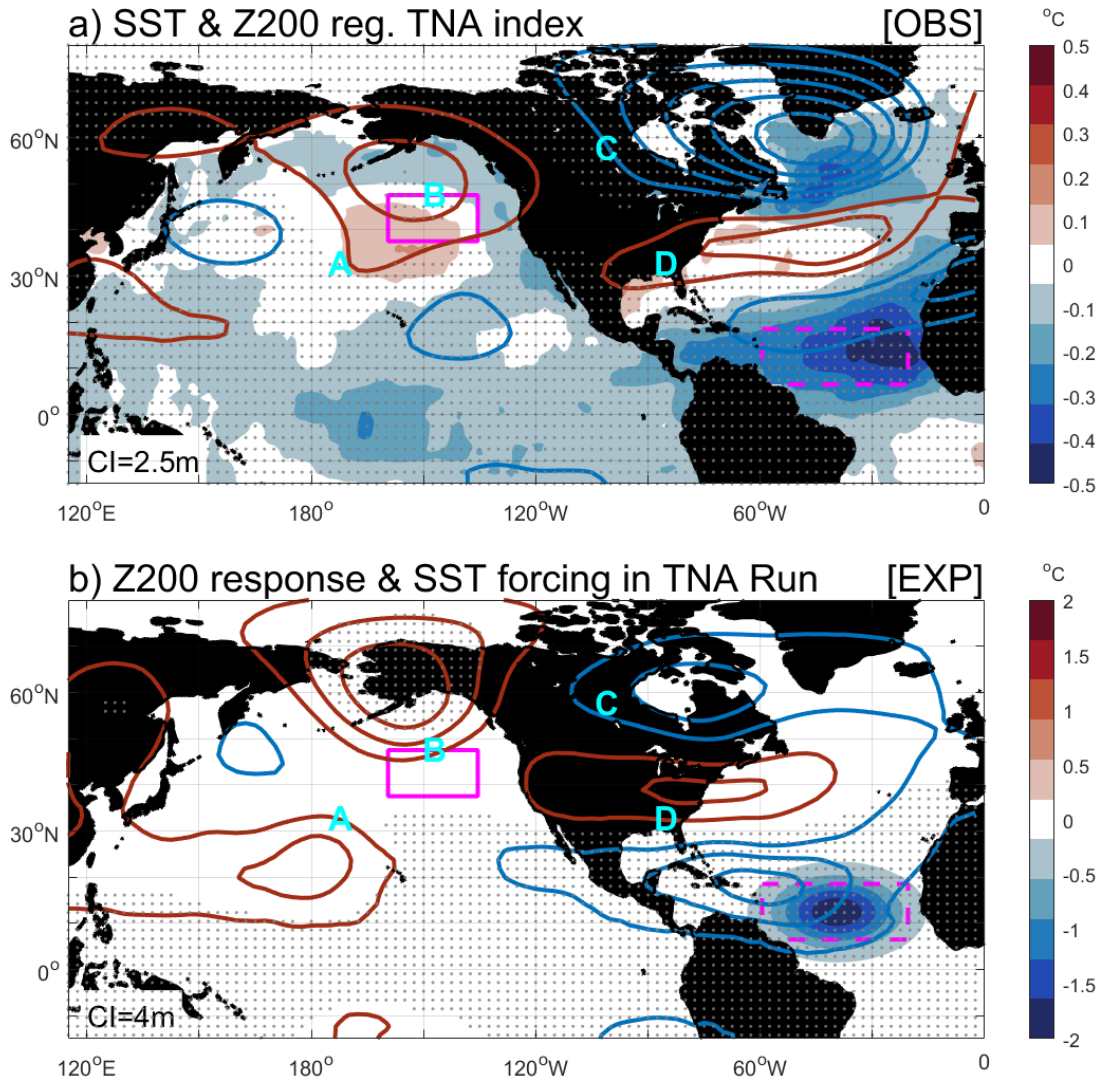
82



83

84 **Figure S4. Seasonal impact of SEP and TCP on atmospheric circulation.** Regression of 200  
 85 hPa geopotential height (Z200) anomalies onto the negative SEP (columns 1–2) and TCP  
 86 (columns 3–4) indices, shown for observations (odd-numbered columns) and model responses  
 87 to forced SEP and TCP perturbations (even-numbered columns), across the four seasons (DJF,  
 88 MAM, JJA, SON from top to bottom). Magenta boxes indicate the Gulf of Alaska (GOA) region;  
 89 green boxes mark the SEP (left) and TCP (right) regions.

90

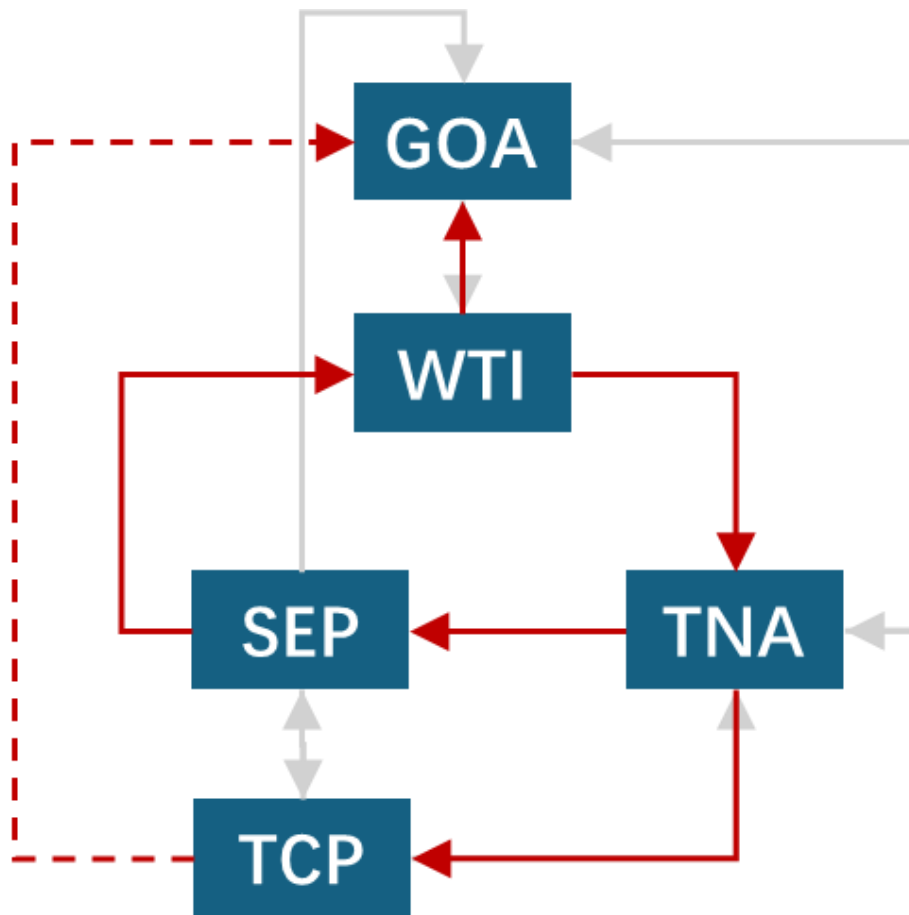


91

92 **Figure S5. Atmospheric circulation response to TNA cooling.** (a) Regression of 200 hPa  
 93 geopotential height (Z200; contours, m) and sea surface temperature (SST; shading, °C) onto  
 94 the negative TNA index, inverted for visual consistency with the TNA model experiment. (b)  
 95 Z200 response from the forced TNA model run, with a prescribed Gaussian SST anomaly  
 96 (shading) in the TNA region. Magenta boxes indicate the Gulf of Alaska (GOA; solid) and  
 97 TNA (dashed) regions. Wave train centers A–D correspond to those identified in Figure 1b.  
 98 Gray dots denote Z200 anomalies significant at the 95% confidence level.

99

100

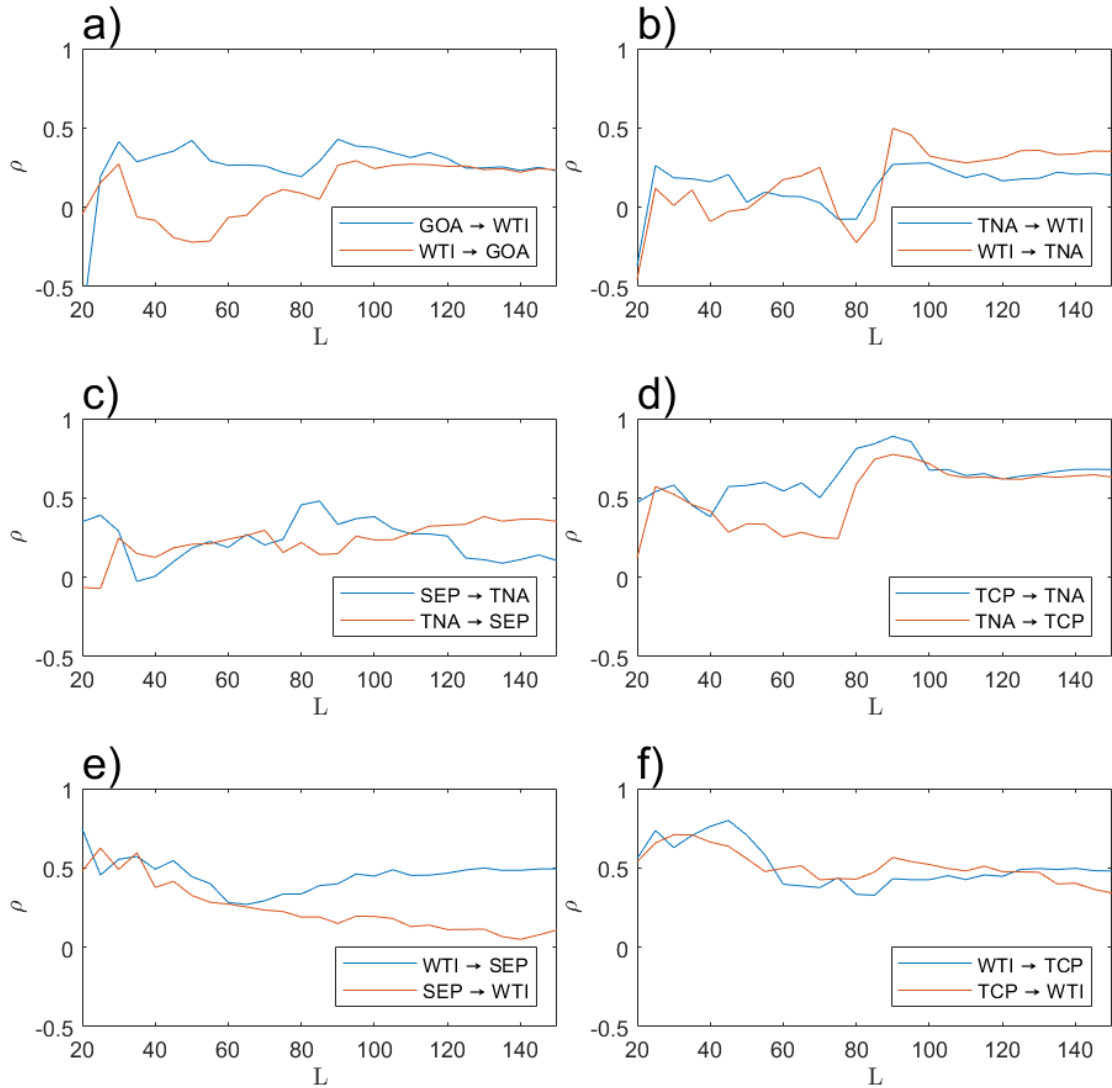


101

102 **Figure S6. Interaction Network Based on Granger Causality Test.** Network diagram  
 103 showing causal relationships between key components of the Pacific-Atlantic feedback loop.  
 104 Solid arrows indicate statistically significant ( $p < 0.05$ ) Granger Causality relationships, while  
 105 dashed arrows show theoretically important but non-significant pathways ( $p > 0.05$ ). Each  
 106 arrow means that past values of the source variable help predict future values of the target  
 107 variable beyond what can be explained by the target's own past values. Results are derived from  
 108 the Granger Causality tests in Table S1. The red arrows highlight our proposed feedback loop  
 109 where ascending motion in the subtropical eastern Pacific (SEP) triggers the WTI, which  
 110 induces tropical North Atlantic cooling (TNA), ultimately feeding back to promote renewed  
 111 ascending motion in the Pacific (TCP & SEP). The direct relationship between the WTI and  
 112 Gulf of Alaska warming (GOA) is also confirmed.

113

114



115

116

**Figure S7. Convergent Cross Mapping Analysis Supporting Trans-Basin Feedback**

117

**Relationships.** Cross-mapping skill ( $\rho$ ) as a function of library size ( $L$ ) for key variable pairs

118

in the proposed Pacific-Atlantic feedback loop. Each panel shows bidirectional testing. The

119

analysis reveals significant convergent relationships that support key components of our

120

proposed feedback mechanism: (a) GOA  $\rightarrow$  WTI showing clear convergence, (b) WTI  $\rightarrow$  TNA

121

demonstrating strong causal relationship, (c) TNA  $\rightarrow$  SEP indicating Atlantic feedback to

122

Pacific, and (d) TNA  $\rightarrow$  TCP showing similar Atlantic influence. Panels (e) and (f) show weaker

123

or non-convergent patterns for WTI  $\leftrightarrow$  SEP and WTI  $\leftrightarrow$  TCP relationships. Convergent

124

behavior—characterized by increasing  $\rho$  values with larger library sizes—indicates genuine

125

causal relationships in the climate system. These results provide nonlinear validation for the

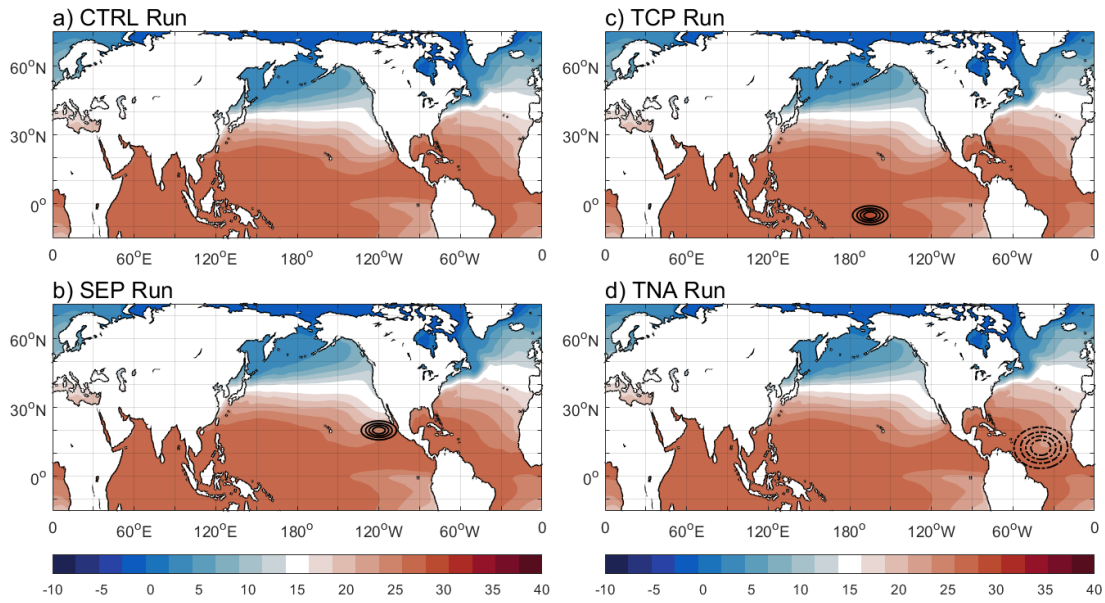
126

core pathways in our trans-basin feedback mechanism identified through Granger Causality

127

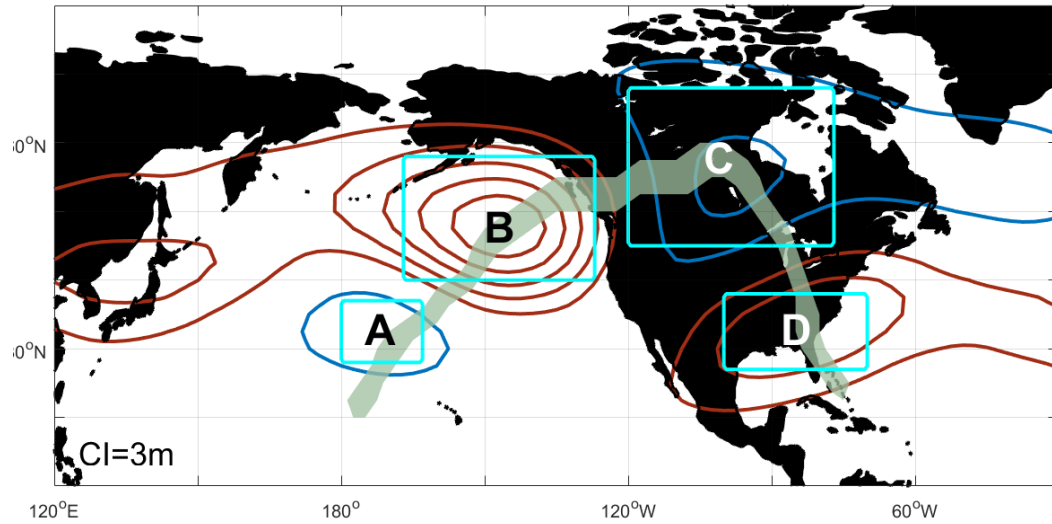
analysis.

128



129  
 130  
 131  
 132  
 133  
 134  
 135  
 136  
 137  
 138

**Figure S8. SST Forcing in AGCM CAM5 Experiments.** Annual mean SSTs for CTRL Run (a), SEP Run (b), TCP Run (c), and TNA Run (d). Contours show Gaussian SSTA at 0.2°C intervals (solid for positive, dashed for negative values). The SEP Run and TCP Run use e-folding radius of 3.5° in the north-south direction and 10.6° in the east-west direction, with a 2°C peak strength at center. The TNA Run uses e-folding radius of 7.5° north-south and 15.5° east-west, with a -2°C peak strength at center.



139

140 **Figure S9. Wave Train Track Identification.** Z200 anomalies regression onto GOA index

141 (1871-2022), from Figure 1b. The green area marks the wave train track along steepest Z200

142 gradients. Cyan boxes mark wave centers A-D corresponding to those in Figure 1b.